Differential activity and selectivity of N-terminal modified CXCL12 chemokines at the CXCR4 and ACKR3 receptors

Agnieszka Jaracz-Ros, Guillaume Bernadat, Pasquale Cutolo, Carmen Gallego, Martin Gustavsson, Erika Cecon, Françoise Baleux, Irina Kufareva, Tracy M Handel, Françoise Bachelerie, et al.

HHS Public Access

Author manuscript

J Leukoc Biol. Author manuscript; available in PMC 2020 October 07.

Published in final edited form as:

J Leukoc Biol. 2020 June ; 107(6): 1123–1135. doi:10.1002/JLB.2MA0320-383RR.

Differential activity and selectivity of N-terminal modified CXCL12 chemokines at the CXCR4 and ACKR3 receptors

Agnieszka Jaracz-Ros[1,*], **Guillaume Bernadat**[2,*], **Pasquale Cutolo**[1], **Carmen Gallego**[1], **Martin Gustavsson**[3,‡], **Erika Cecon**[4], **Françoise Baleux**[5], **Irina Kufareva**[3], **Tracy M. Handel**[3], **Françoise Bachelerie**[1,*,†], **Angélique Levoye**[6,7,*,†]

[1]Université Paris-Saclay, INSERM, Inflammation, Microbiome and Immunosurveillance, 92140, Clamart, France.

[2]Université Paris-Saclay, CNRS, BioCIS, 92290, Châtenay-Malabry, France

[3]Skaggs School of Pharmacy and Pharmaceutical Sciences, University of California, San Diego, 9500 Gilman Drive, La Jolla, CA 92093, USA.

[4]Université de Paris, Institut Cochin, CNRS, INSERM, F-75014 Paris, France.

[5]Institut Pasteur, Unité de Chimie des Biomolécules, CNRS UMR 3523, 28 rue du Dr Roux, 75724 Paris Cedex 15, France.

[6]Université de Paris, PARCC, INSERM, F-75015 Paris, France.

[7]Université Sorbonne Paris Nord, Bobigny, France.

Abstract

Chemokines play critical roles in numerous physiological and pathological processes through their action on seven-transmembrane (TM) receptors. The N-terminal domain of chemokines, which is a key determinant of signaling *via* its binding within a pocket formed by receptors' TM helices, can be the target of proteolytic processing. An illustrative case of this regulatory mechanism is the natural processing of CXCL12 that generates chemokine variants lacking the first two N-terminal residues. While such truncated variants behave as antagonists of CXCR4, the canonical G protein-coupled receptor of CXCL12, they are agonists of the atypical chemokine receptor 3 (ACKR3/

[†]Address correspondence to: Dr. Françoise Bachelerie, INSERM UMR 996, Inflammation Microbiome and Immunosurveillance, Université Paris-Saclay, 32 rue des Carnets, 92140 Clamart, France, Tel: +331 41 28 80 05, Fax: +331 46 32 79 93. francoise.bachelerie@universite-paris-saclay.fr or Dr. Angélique Levoye, INSERM UMR 970, Regenerative Therapies For Cardiac And Vascular Diseases, 56 rue Leblanc, 75737 Paris Cedex 15, France Tel: +33153987980, Fax: +330153987951. angelique.levoye@inserm.fr.

[*]These authors contributed equally to this work.

[‡]Present address: Department of Biomedical Sciences, University of Copenhagen, Blegdamsvej 3, 2200 Copenhagen, Denmark.

AUTHORSHIP

AJ-R and AL designed, performed and analyzed *in vitro* BRET and HTRF-based experiments and produced the figures and tables. PC and CG contributed to the internalization assays. GB provided expertise in MD simulations and with AJ-R conceived and performed the MD analyses. EC provided expertise in molecular pharmacology and analyses of cAMP and competitive binding analysis. F. Baleux performed chemokine synthesis. IK, MG and TH built the molecular model of ACKR3-CXCL12 complex and shared the atomic coordinates. F. Bachelerie conceived and supported the study. AL and F. Bachelerie wrote the initial manuscript, TH, IK, AJ-R and GB edited the draft and the other authors contributed to editing it in its final form. All authors approved the final version of the MS.

DISCLOSURE

The authors declare that they have no conflict of interest.

CXCR7), suggesting the implication of different structural determinants in the complexes formed between CXCL12 and its two receptors. Recent analyses have suggested that the CXCL12 N-terminus first engages the TM helices of ACKR3 followed by the receptor N-terminus wrapping around the chemokine core. Here we investigated the first stage of ACKR3-CXCL12 interactions by comparing the activity of substituted or N-terminally truncated variants of CXCL12 toward CXCR4 and ACKR3. We showed that modification of the first two N-terminal residues of the chemokine (K1R or P2G) does not alter the ability of CXCL12 to activate ACKR3. Our results also identified the K1R variant as a G protein-biased agonist of CXCR4. Comparative molecular dynamics simulations of the complexes formed by ACKR3 either with CXCL12 or with the P2G variant identified interactions between the N-terminal 3–5 residues of CXCL12 and a pocket formed by receptor's TM helices 2, 6 and 7 as critical determinants for ACKR3 activation.

Summary sentence:

Three to five N-terminal residues of CXCL12 are critical for binding to ACKR3 and required for activation of both CXCR4 and ACKR3

Keywords

ACKR3; CXCR4; CXCL12; chemokine variants; GPCR signaling; pluridimensional efficacy

Subject Category:

Receptors; Signal Transduction and Genes

INTRODUCTION

Chemokines are small secreted proteins that direct cell migration through their cognate G-protein coupled receptors (GPCRs) [1]. Originally isolated from murine bone marrow stromal cells [2], the chemokine, CXCL12, is now known to be expressed in a wide range of tissues and upregulated by inflammatory cues [3]. Thus, besides its function in regulating leukocyte trafficking, CXCL12 also plays a broader role in regulating cell positioning in health as well as in pathological conditions including chronic inflammation and cancers [4]. CXCL12 is the ligand of CXCR4 and ACKR3, the latter of which also binds to CXCL11, a ligand that is shared with CXCR3 [5–7]. While CXCR4 is ubiquitously expressed in various cells and tissues, the expression pattern of ACKR3 remains poorly understood, because its predominantly intracellular localization makes detection of ACKR3 in native tissues challenging [8]. ACKR3 expression is usually low at steady state and highly upregulated in pathological contexts; this includes several types of cancers where ACKR3 can be detected in the primary tumor as well as in the tumor-associated vasculature suggesting its role in tumorigenesis and cancer metastasis [9–11]. Moreover, like CXCR4, ACKR3 is essential to mouse development, but both receptors perform complementary and non-redundant functions in response to CXCL12 [12–14]. Although in contrast to canonical chemokine receptors, ACKR3 does not activate G proteins [5, 7, 15], it can directly engage β-arrestins and trigger arrestin-mediated signaling upon CXCL12 binding [6, 16]. Several lines of evidence have also underscored the regulatory role of ACKR3 in the CXCL12/CXCR4

signaling axis by modifying chemokine gradients through scavenging of CXCL12 [14, 15, 17–22]. In addition, oligomerization of ACKR3 and CXCR4 has been shown to modulate CXCR4-mediated signaling [12, 15, 23, 24] although this process is still awaiting direct evidence in endogenous settings. With CXCR4, the physiological relevance of dimerization suggested by crystal structures [25], and by its reported partitioning into microclusters in native tissues [26], might be required for maximal response to CXCL12 [27]. These interrelated functions of CXCR4 and ACKR3 raise questions about the underappreciated binding and signaling peculiarities of CXCL12 in relation to each of its two receptors. A two-site, two-step model for CXCR4-CXCL12 interactions was proposed, which results in the introduction of the chemokine N-terminus within the CXCR4 transmembrane (TM) cavity and triggers receptor activation [28–30]. The crystal structure of CXCR4 and receptor mutagenesis confirmed this model [25, 31, 32], and functional experiments revealed the critical role of the two first CXCL12 N-terminal residues (Lysine (K)1 and Proline (P)2) for CXCR4 activation [28, 33–35]. For the ACKR3-CXCL12 complex, recent analyses revealed a contrasting pattern where the P2 residue is not essential for ACKR3 activation [36] and more distant residues of CXCL12 (*e.g.* Tyrosine (Y)7) may be important instead [37]. Here we compared the pharmacological and signaling properties of N-terminally modified CXCL12 variants in relation to CXCR4 and ACKR3. We used two substituted (K1R and P2G) and two truncated (4–67 and 5–67) variants of CXCL12, previously described as CXCR4 antagonists [28, 38, 39]. Our data indicate that neither K1 nor P2 is necessary for promoting ACKR3-dependent β-arrestin recruitment or receptor internalization in living cells. They also reveal that the CXCL12 K1R variant behaves as a partial agonist for CXCR4-dependent inhibition of cAMP production. Finally, molecular dynamics analyses allow to propose that the interactions between the three N-terminal residues (Valine (V)3, Serine (S)4, Leucine (L)5) of CXCL12 and the TM2, 6 and 7 domains of ACKR3 represent critical determinants for receptor activation.

MATERIALS AND METHODS

Chemokine synthesis

Wild-type CXCL12, CXCL12 4–67, CXCL12 5–67, CXCL12 K1R, CXCL12 P2G were synthesized by the Merrifield solid-phase method as described previously [40].

Reagents and Plasmids

CXCL11 was obtained from Almac sciences. AMD3100 and T134 were from the NIH AIDS Research & Reference Reagent Program. Tag-lite® binding assay (CXCL12 labeled with a red fluorescent probe (red-CXCL12), the Tag-lite labeling medium and SNAP-Lumi4-Tb) were developed by Cisbio Bioassays (Bagnols-sur-Cèze, France). Poly-L-ornithine (MW of 30,000–70,000 Da) and forskolin were from Sigma-Aldrich (Saint Louis, MO).

The Rluc-β-arrestin 2 and Rluc8-β-arrestin 2-YPet expression vectors, previously reported [41, 42] were a gift from Dr. M.G. Scott (Institut Cochin, Paris) and Dr. C. Couturier (INSERM U761, Université de Lille 2, France), respectively. The expression vectors

encoding the ACKR3 and CXCR4 receptors C-terminally tagged with YFP (ACKR3-YFP and CXCR4-YFP) have been previously described [15].

Cell culture and transfection

HEK293T cells were grown in culture medium (DMEM supplemented with 10 % (v/v) FBS, 4.5 g/L glucose, 100 U/mL penicillin, 0.1 mg/mL streptomycin, 1 mM glutamine, 20 mM Hepes) (all reagents are from Invitrogen SARL, Cergy Pontoise, France). HEK293 cells stably expressing the SNAP-tag-fused CXCR4 or ACKR3 receptors (ST-CXCR4 or ST-ACKR3 cells) were provided by Cisbio Bioassay and were grown in culture medium supplemented with 0.6 μg/mL geneticin (Invitrogen SARL, Cergy Pontoise, France). Transient transfections were performed using the transfection reagent FuGene 6 (Roche, Basel, Switzerland) or Lipofectamine 2000 (Invitrogen, CA, USA) according to the manufacturer's protocol.

Homogenous Time-Resolved Fluorescence (HTRF)-based binding assay

The protocol has been adapted from Zwier et al. [43]. Briefly, Lumi4-Tb-labelled-frozen ST-CXCR4 or ST-ACKR3 cells were thawed quickly at 37°C, suspended in the Tag-lite labeling medium and dispatched into a black 384-well plate at a density of 10^4 cells per well. Competition experiments were performed by incubating ST-CXCR4- or ST-ACKR3-cells with a fixed concentration of red-CXCL12 (12.5 nM or 6.25 nM, respectively, according to the respective K_d, see Fig. S1) in presence of increasing concentrations of the indicated ligands for 1 hour at room temperature. Signal was detected using fluorescence microplate reader Rubystar (BMG Labtech, Offenburg, Germany) equipped with a HTRF optic module allowing a donor (terbium) excitation at 337 nm and a signal collection both at 620 nm and 665 nm, wavelengths corresponding to the total donor emission and to the FRET signal, respectively. The signal was collected using the following time-resolved settings: delay 50 μs and integration time 400 μs. HTRF ratios correspond to the ratio between acceptor (665 nm) and donor signal (620 nm) and multiplied by 10000. Concentration-responses curves were fitted with a non-linear regression dose–response "log [inhibitor] versus response (three parameters)" using Prism 7.0 software (GraphPad Inc., San Diego, CA) to provide IC_{50} and pIC_{50}. The K_i values for ligands were calculated from binding competition experiments according to the Cheng and Prusoff equation: $K_i = IC_{50} \times K_d/(K_d + [L])$, where IC_{50} is the concentration of ligands leading to half-maximal inhibition of specific binding, K_d is the affinity of fluorescent chemokine for the receptor studied, and [L] is the concentration of the red-CXCL12 present in the assay. Data are mean ±SEM expressed as % of maximal response for each ligand.

Receptor internalization assay

Internalization assays for CXCR4 and ACKR3 were performed in 96-well culture cell plates using ST-CXCR4 or ST-ACKR3 cells as previously described [44]. Briefly, upon SNAP Lumi4-Tb labeling, internalization experiments were performed by incubating cells with Tag-lite labeling medium, either alone or containing ligands (CXCL12, CXCL11, CXCL12-derivatives or small molecules AMD3100 and T134) in the presence of fluorescein. Typically, in plates containing SNAP-Lumi4-Tb-labeled cells, 10 μL of medium containing ligands at saturating concentration was added, immediately followed by the addition of 80

µL of fluorescein (for final in-well concentrations of 1 µM ligand and 20 µM fluorescein). Plates were incubated for 1 hour at 4°C and signals were detected using fluorescence microplate reader (Envision, Perkin Elmer) at 37°C. DERET ratios were obtained by dividing the donor signal (620 nm) by the acceptor signal (520 nm) and multiplying this value by 10000.

β-Arrestin recruitment

HEK293T cells (5×10^5 cells/well) were seeded into 6-well plates in culture medium and transfected using the transfection reagent FuGene 6 (Roche, Basel, Switzerland) or Lipofectamine 2000 (Invitrogen, CA, USA) according to the manufacturer's protocol. Cells were transiently co-transfected with 0.1 µg of Rluc-β-arrestin 2 or Rluc8-β-arrestin 2-YPet and 1 µg of receptor-YFP expression vectors as previously described [15, 42]. The total amount of cDNA was kept at 2 µg cDNA/well by addition of an empty vector. Forty-eight hours after transfection, cells were washed in PBS, detached in PBS-EDTA and suspended in 300 µL of PBS. Cells were distributed into a white 96-well plate (35 µL/well, Optiplate, PerkinElmer) at a density of 400 000 cells per well. For dose-response experiments, cells were incubated with ligands at the indicated concentrations for 10 min at 37°C before adding 5 µM of coelenterazine h (Interchim, Montluçon, France), as previously reported [15]. For the β-arrestin biosensor, cells were incubated with 1 µM ligands for 20 min at 37°C before adding 5 µM of coelenterazine h. BRET values were collected using the Mithras LB940 reader (Berthold Biotechnologies, Bad Wildbad, Germany) that allows the sequential integration of luminescence signals detected with two filters settings (Rluc filter, 485 ± 20 nm; and YFP filter, 530 ± 25 nm). BRET signals were measured and expressed as the ratio of the light emitted by the acceptor (YPet) divided by the light emitted by the donor (Rluc8). Averaged BRET values were plotted against log [ligand], and the resulting concentration-responses curves were fitted with a non-linear regression dose–response "log [ligand] versus responses" with variable slope using Prism 7.0 software (GraphPad Inc., San Diego, CA) to provide the E_{max}, EC_{50} and pEC_{50} values. The E_{max} of CXCL12 variants was expressed as the percentage of the maximal response to 1 µM CXCL12 which was set to 100%.

cAMP measurements—Cyclic AMP (cAMP) levels were determined by HTRF using the Cisbio "cAMP dynamic" kit according to the manufacturer's instructions. Briefly, native cAMP produced by cells is competing with cryptate-labeled cAMP for binding to monoclonal d2-labeled anti-cAMP antibody. An increase in intracellular cAMP leads to disruption of FRET signal, whereas a decrease in intracellular cAMP results in higher FRET signal. The cAMP assays were performed on cryopreserved ST-CXCR4 cells that were rapidly thawed at 37°C and resuspended in cell suspension buffer (HBSS, 20 mM HEPES, 0.1% fatty acid–free BSA). Cells were seeded into a 384-well plate and treated with ligands diluted in stimulation buffer (HBSS, 20 mM HEPES, 500 µM IBMX, 6.5 µM forskolin). After 1 hour at room temperature, HTRF detection reagents were added to the cells (5 µL) and signals were analyzed with an Envision (BGM Labtech, Offenburg, Germany). Signals emitted at 665 and 620 nm were collected using time-resolved settings for the donor (1500 µs delay, 1500 µs reading time) and acceptor (150 µs delay, 400 µs reading time). Ratio 665/620 (R) was obtained by dividing the acceptor signal (665 nm) by the donor signal (620 nm) at a chosen concentration of the ligand and multiplying this value by 10000. Data are

expressed as “Inhibition of cAMP production (% of maximal CXCL12 response)” and were calculated using the following formula: $[(Rt - Rmin)/(Rmax - Rmin)] \times 100$ where Rt corresponds to the ratio observed at a chosen concentration. A nonlinear regression using a sigmoidal dose response model with three parameters was used to fit the data using Prism 7.0 GraphPad software (Inc., San Diego, CA) to provide the E_{max}, and (pIC_{50}) values. The signal obtained for each ligand was reported as the percentage of the maximal response to 1 μM CXCL12, which was set to 100%.

MD simulations of ACKR3 in complex with WT CXCL12 or CXCL12 P2G

The structure of a starting conformation of the complex between CXCL12 bearing the P2G mutation and ACKR3 was obtained by side-chain replacement on the model from reference [37] using UCSF Chimera v1.11 software package [45]. Both this mutant complex and its WT counterpart were subjected to a 50 ns-long molecular dynamics in a solvated lipid bilayer environment (1-palmitoyl-2-oleoyl-sn-glycero-3-phosphocholine). First, the extracellular and cytoplasmic domains of the complexes were solvated with a shell of water molecules using the SOLVATE program [46]. Lipids were then loosely arranged around the TM domain by repetition and truncation of a pre-equilibrated periodic patch of POPC molecules using the Membrane Builder plug-in of the VMD v1.9.2 software package [47]. Extra water molecules were then added so as to fill in a ~90×90×115 Å periodic simulation box, then misplaced water molecules were deleted and random water molecules were replaced by sodium and chloride ions in order to reach electric neutrality and a 150 mM salt concentration. Topologies for the chemokine and receptor subunits as well as the lipids bilayer were generated in the CHARMM22 [48, 49] and CHARMM27 [50, 51] all-atom protein and lipid force fields respectively, in combination with TIP3P water model [52]. The systems were then energy-minimized and progressively equilibrated by running a molecular dynamics simulation of the lipid tails exclusively for 0.5 ns. Simulation was continued for 0.5 ns while constraining the protein with harmonic forces but freeing the whole lipids and keeping water molecules outside the bilayer. Eventually, the system was further equilibrated without any constraint for another 0.5 ns using Langevin dynamics and modified Nosé-Hoover pressure control [50, 53] as implemented in NAMD v2.12 software package [54, 55]. Production was conducted for 50 ns on each complex under the same conditions. Atom coordinates were saved every 2 ps for subsequent trajectory analysis. For every frame of both trajectories and each of the first five N-terminal residues of the chemokine, residues of ACKR3 possessing an atom located closer than 0.4 Å to the residue of interest were listed. Consecutive frames were then binned by groups of 500 and the number of times during which a contact exists between pairs of residues being considered was calculated within each bin. These values were finally plotted as a function of time under the form of colored bars. Depictions of the structure of molecular dynamics endpoint for each complex were prepared and rendered with UCSF Chimera v1.11 software package [45].

Statistical analysis

Data and statistical analyses were performed using Prism software version 7.0 (GraphPad Inc., San Diego, CA). Data from at least three independent experiments performed in triplicate are expressed as mean ± SEM. Unpaired two-tailed t-test was used to analyze the difference in pIC_{50} values in cAMP assay for each CXCL12 variant using the WT CXCL12

as reference. For BRET experiments with β-arrestin biosensor, β-arrestin recruitment and competitive binding assay one-way analysis of variance (ANOVA) with Dunnett's multiple comparison test with WT CXCL12 as control was applied.

RESULTS

CXCL12 variants differently bind to CXCR4 and ACKR3

Using a HTRF-based or Tag-Lite ligand binding assay [43], we compared the binding of CXCR4 and ACKR3 to different chemically synthesized CXCL12 variants, including two N-terminally truncated (4–67 and 5–67) and two substituted (K1R and P2G) variants (Fig. 1). Dissociation constants (K_d) of CXCL12 for CXCR4 and ACKR3 were determined by direct saturation binding experiments using fluorescent CXCL12 and donor labeled SNAP-Tagged CXCR4 or ACKR3 stably expressed in HEK293 cells (Table 1, Fig. S1). We then investigated the ability of WT CXCL12 and its variants to displace the binding of the fluorescent chemokine using a HTRF competitive binding assay (Fig. 2). We first confirmed the higher affinity of CXCL12 for ACKR3 (Fig 2B) as compared to CXCR4 (Fig. 2A) [5–7, 56] and found that this feature was maintained for the CXCL12 variants K1R and P2G: although their inhibition constants were altered, the relative affinity of the variants to the two receptors remained the same. By contrast, truncated CXCL12 variants 4–67 and 5–67 were much less potent in displacing red-CXCL12 binding to ACKR3 as compared to CXCR4, which hampered quantification of their binding affinities for ACKR3 (Table 1). These findings confirm the importance of the first five N-terminal residues of CXCL12 for the interaction with CXCR4 [28, 57] and indicate a more prominent role of the third and fourth N-terminal residues of CXCL12 than the first two residues in binding to ACKR3.

CXCL12 K1R is a partial agonist of CXCR4-mediated cAMP inhibition

Efficacy of various ligands towards their receptors can depend upon the effector system considered, a phenomenon referred as functional selectivity or biased agonism [58]. Ligands might thus display different potencies and efficacies toward their receptors depending on the signaling pathways considered. A canonical example is given by a β-blocker propranolol, which behaves as an inverse agonist on adenylate cyclase signaling cascade but an agonist on ERK1/2 pathway for both β_1 and β_2 adrenergic receptors [59]. Here we investigated the ability of CXCL12 K1R and CXCL12 P2G variants to activate Gi protein-dependent signaling downstream of CXCR4, given that they retained binding affinities in the range of their WT counterpart. We determined that CXCL12 K1R was able to inhibit forskolin-stimulated cAMP accumulation downstream of CXCR4, but with a reduced efficacy as compared to WT CXCL12 (Fig. 3). As expected, neither CXCL11 nor CXCR4 antagonists AMD3100 or T134 were able to elicit a response. Efficacy of each compound based on its maximal effective concentration was determined from dose-response curves (Fig. 3). This data indicated that the CXCL12 K1R variant harbors a similar potency, but a reduced efficacy (E_{max} of 60%) as compared to the WT chemokine (Table 2) suggesting that it behaves as a partial agonist of this Gi protein-dependent signaling pathway.

CXCL12 K1R and P2G variants induce ACKR3 internalization

The binding affinity of N-terminally truncated variants of CXCL12 to CXCR4 does not necessarily correlate with their ability to activate the receptor. This is illustrated by the CXCL12 P2G variant that acts as an antagonist while retaining a binding affinity not too dissimilar from the WT chemokine [25, 28]. Additionally, none of the CXCL12 variants including K1R were able to induce CXCR4 internalization above the background (Fig. 4A). In contrast, internalization of ACKR3 in response to CXCL12 variants correlated with their binding affinity for ACKR3 (Table 1, Fig. 2): the K1R and P2G mutant retained the ability to induce receptor internalization similar to WT CXCL12, while the truncated variants 4–67 and 5–67 were inactive (Fig. 4B).

CXCL12 N-terminal residues V3 and S4 are necessary for ACKR3-mediated β-arrestin recruitment

We then investigated whether CXCL12 K1R and P2G variants can promote β-arrestin 2 recruitment to CXCR4 and ACKR3. In the case of CXCR4, β-arrestin 2 recruitment is believed to be necessary for receptor internalization [60], whereas the relationship of ACKR3 internalization with β-arrestin 2 recruitment to this receptor is still debated [21, 22, 61]. In our experiments, the ability of chemokine variants to promote β-arrestin 2 recruitment to both receptors was in agreement with the internalization data. In particular, β-arrestin 2 recruitment to CXCR4 was promoted only by WT CXCL12 (Fig. 5A), whereas in the case of ACKR3, both K1R and P2G variants were able to promote β-arrestin 2 recruitment in contrast to the CXCL12 truncated mutants (Fig. 5B). Analyses of dose-response curves indicated that the CXCL12 K1R mutant promoted the recruitment of β-arrestin 2 to ACKR3 with potency and efficacy comparable to that of the WT chemokine (Table 3). The P2G variant also promoted β-arrestin 2 recruitment, albeit with weaker potency and efficacy as compared to WT CXCL12 (Fig 5B, Table 3). Next, we investigated whether the CXCL12 K1R and P2G variants were able to promote receptor-dependent intramolecular conformational changes of β-arrestin 2, which is a reliable indicator of arrestin activation by the receptor [62]. Using an intramolecular BRET approach, we detected a measurable signal in CXCR4-expressing cells only in response to WT CXCL12 (Fig. 5C). However, for ACKR3-expressing cells, a comparable signal was detected in response to WT CXCL12 and to the two CXCL12 N-terminal mutants; the signal was abrogated by the N-terminal truncations 4–67 and 5–67 of CXCL12 (Fig. 5D). These results point to the third and fourth CXCL12 N-terminal residues (V3 and S4) as important determinants for the binding of CXCL12 to ACKR3 and activation of the receptor.

Conformational dynamics of ACKR3-CXCL12 complexes revealed the importance of CXCL12 N-terminal residues 3–5

In order to investigate the hypothesis that residues V3 and S4 are important for ACKR3 activation and confirm that the first two residues (K1 and P2) are not essential, we compared MD simulations of ACKR3 in complex with CXCL12 and with the P2G variant. The simulations with the ACKR3-CXCL12 P2G complex were intended to highlight the interactions between ACKR3 and the V3, S4, L5 CXCL12 residues. Starting from these initial conformations [37], RMSD as a function of time (50ns) indicated that the P2G

mutation affects the overall conformation of the ACKR3-CXCL12 complex although both complexes reached equilibrated tertiary structures during the 50 ns trajectories (Fig. S2A). Moreover, RMSF analysis confirmed that the chemokine N-terminus becomes more flexible (~20% increase) as a consequence of the P2G mutation, suggesting that its conformation does not play a dominant role in ACKR3 activation (Fig. S2B). We then examined the contacts between ACKR3 and the V3 N-terminal residue of CXCL12 or of the P2G variant. These analyses illustrated a striking superposition of the tertiary structures formed by ACKR3 in complex with CXCL12 and the P2G variant (Fig. 6A) as a consequence of the conservation over time of the strong contacts and hydrophobic interactions established between receptor residues and the V3 of both forms of the chemokine (Fig. 6B). More specifically, the strong contacts identified between V3 of WT CXCL12 and ACKR3 residues ($W100^{2.60}$, $Q301^{7.39}$, $L297^{7.35}$ and $H298^{7.36}$ (Ballesteros-Weinstein numbering in superscript [63])) were maintained for the P2G variant. Of interest, $W100^{2.60}$, $Q301^{7.39}$ residues were reported to be important for CXCL12-induced β-arrestin recruitment to ACKR3 [61]. This is illustrated in Figure 6B by similar strength of interactions, which corresponds to the proportion of time during which a contact exists between ACKR3 and CXCL12 residues. Such conservation of the positioning of the CXCL12 V3 within a binding site involving ACKR3 residues localized in TM7 and TM2 dramatically contrasted with the destruction of strong hydrophobic interactions and hydrogen bonds established between the first N-terminal K1 residue of CXCL12 and ACKR3 as a consequence of the P2G mutation (Fig. S3). Along these lines, MD simulations presented in Figure 7 (see also Fig. S4) also support the importance of CXCL12 N-terminal residues S4 and L5 together with V3 in establishing strong contacts with ACKR3. They engaged ACKR3 residues $Y268^{6.51}$ and $D275^{6.58}$ (Fig. 7A), through strong hydrogen bonds with the backbone regions of CXCL12 S4 and L5 in both WT CXCL12 and the P2G variant (Fig. 7B and 7C). Collectively, MD simulations of ACKR3-CXCL12 complexes allowed identification of a cluster formed by the N-terminal V3, S4 and L5 residues of CXCL12 that establish strong interactions with residues of ACKR3 and are likely involved in the activation of the receptor.

DISCUSSION

Models of the receptor-chemokine complex based on crystal structures of CXCR4 [25, 31] and mutational analyses [25, 31, 32], indicate that beyond the two main chemokine recognition sites (CRS), which implicate the core (CRS1) and the N-terminus of the chemokine (CRS2), a continuous interaction interface exists between chemokines and their receptors. CRS2 interactions in the receptor TM helices are believed to be mostly important for receptor activation while CRS1 interactions in the receptor N-terminus contribute primarily to chemokine binding [30]. Recent mutational analyses and ligand association/dissociation kinetics have suggested that these two stages of interactions are interdependent within the ACKR3-CXCL12 complex with the N-terminus of CXCL12 first engaging the TM helices of the receptor followed by the receptor N-terminus wrapping around the chemokine core [64]. Here we examined in detail the first stage of CXCL12-ACKR3 interactions, by comparing the contribution of the N-terminus of CXCL12 to ACKR3 binding and activation to that of CXCR4. Our findings indicate that the binding of CXCL12 to ACKR3 is critically dependent on the integrity of the first three residues of the chemokine

whereas the 4–67 truncated CXCL12 variant remains able to bind CXCR4 as previously shown [28, 65]. However, and according to the two-step/two-site model for CXCL12-CXCR4 interaction, this truncation resulted in a dramatic loss of CXCL12's ability to activate CXCR4. Of importance, we identified the CXCL12 K1R variant as a ligand that still displays the ability to modulate cyclic AMP downstream CXCR4 although with a reduced efficacy as compared to the WT CXCL12. However, this variant could not promote either CXCR4-dependent calcium release or β-arrestin recruitment or receptor internalization, as also shown by others [28, 66], suggesting that it behaves as a biased agonist for CXCR4-dependent inhibition of cAMP. MD simulations of CXCR4/K1R complexes and extended analyses of G protein-dependent pathways downstream CXCR4 could provide further support with regard to the biased agonist behavior of this N-terminal modified chemokine.

In contrast to this situation, the K1R but also the P2G variant remain capable of promoting ACKR3-mediated β-arrestin recruitment, considered here as receptor activation (although β-arrestin-mediated signaling downstream of CXCL12-ACKR3 remains to be demonstrated *in vivo*). This is in agreement with recent observations of the P2G as well as another LRHQ chemokine variant [64]. The slightly decreased potency and efficacy of the P2G variant that others have previously shown for CXCL12 N-terminus-derived peptides encompassing the P2G mutation [36, 56] could arise from the faster dissociation of the P2G variant from ACKR3 compared to WT CXCL12 [64]. The effects of CXCL12 K1R and P2G variants on signaling pathways induced by CXCR4 and ACKR3 reported so far are provided in Table S1. Collectively, our data point to the third and fourth CXCL12 N-terminal residues (V3 and S4) as important determinants for the binding of the chemokine to ACKR3 and activating ACKR3-dependent β-arrestin recruitment and receptor internalization. These results are in line with radiolytic footprinting analyses indicating that the CXCL12 N-terminus contributes to the binding of the chemokine to ACKR3 [37]. Moreover, the 3–68 CXCL12 natural variant, resulting from dipeptidylpeptidase IV CD26-dependent proteolytic cleavage [67], was capable of activating ACKR3, but not CXCR4 [65] indicating that the natural N-terminal cleavage of CXCL12 might confer differential selectively of the chemokine toward its two receptors. The fact that the 3–68 CXCL12 natural variant is only partially active through ACKR3-dependent β-arrestin recruitment as compared to its WT counterpart [65] is possibly due to the positively charged N-terminus of the V3 that would reduce the strength of the interaction of this residue with ACKR3.

MD simulations have strengthened the possibility that V3 serves as a key binding and activation determinant, by identifying strong contacts and hydrophobic interactions between this residue and ACKR3 residues $W100^{2.60}$, $Q301^{7.39}$, $L297^{7.35}$ and $H298^{7.36}$. We propose that the N-terminal V3, S4 and L5 residue cluster of CXCL12 may initially bind to the above-mentioned residues in ACKR3 that are involved in the ACKR3 scavenging function [22, 36, 56, 61, 68]. As suggested by recent data [64], these initial CRS2 contacts are stabilized by interactions between the receptor N-terminus and CXCL12 core (CRS1), indicating that rather than being decoupled, the two sites are actually interdependent. Other atomic-level factors contributing to the interactions of both partners are currently being sought with similar approaches.

Supplementary Material

Refer to Web version on PubMed Central for supplementary material.

ACKNOWLEDGMENTS

This work was supported by grants from Ensemble Contre le SIDA (SIDACTION), the Institut National de la Santé et de la Recherche Médicale (INSERM), GIS-Network for Rare Diseases and the Agence Nationale de Recherches sur le SIDA (ANRS). We thank members of Dr. F. Arenzana-Seisdedos laboratory (Laboratoire de Pathogénie Virale, Institut Pasteur, Paris, France) and Dr. R. Jockers (Institut Cochin, Paris), who provided critical discussion. The authors wish to thank E. Trinquet, N. Gregor and F. Maurin (CisBio International, Marcoule, France) for technical support in HTRF assays. AL was supported by Roux Post-doctoral fellowship from Pasteur Institute. IK and TMH are supported by NIH R01 grants AI118985 and GM117424. CG was supported by MSCA-ITN-2014-ETN - Marie Skłodowska-Curie Innovative Training Networks (ITN-ETN) “ONCOgenic Receptor Network of Excellence and Training” and CG was supported by the Fondation pour la Recherche Médicale (FDT201805005700).

ABBREVIATIONS

ACKR3	Atypical Chemokine Receptor 3
BRET	Bioluminescence Resonance Energy Transfer
CRS1/CRS2	Chemokine recognition site 1/2
CXCL12, CXCL11	C-X-C Motif Chemokine Ligand 11 or Ligand 12
CXCR3	CXC chemokine receptor 3
CXCR4	CXC chemokine receptor 4
DERET	Diffusion Enhanced Resonance Energy Transfer
ECL	Extracellular loops
EC_{50}	Half maximal effective concentrations
FRET	Fluorescence Resonance Energy Transfer
GPCR	G protein-coupled receptor
HEK293	Human embryonic kidney cells
HTRF	Homogenous Time-Resolved Fluorescence
IC_{50}	Half maximal inhibitory concentrations
K_i	Inhibitory constant
K_d	Dissociation constant
MD	Molecular dynamics
Rluc	Renilla reniformis luciferase
RMSD	Root Mean Square Distance

RMSF	Root Mean Square Fluctuation
TM	Transmembrane
YFP	Yellow Fluorescent Protein
WT	Wild type

REFERENCES

1. Zlotnik A and Yoshie O. (2012) The chemokine superfamily revisited. Immunity 36, 705–16. [PubMed: 22633458]
2. Nagasawa T, Kikutani H, Kishimoto T. (1994) Molecular cloning and structure of a pre-B-cell growth-stimulating factor. Proceedings of the National Academy of Sciences of the United States of America 91, 2305–9. [PubMed: 8134392]
3. Murphy PM and Heusinkveld L. (2018) Multisystem multitasking by CXCL12 and its receptors CXCR4 and ACKR3. Cytokine 109, 2–10. [PubMed: 29398278]
4. Janssens R, Struyf S, Proost P. (2018) Pathological roles of the homeostatic chemokine CXCL12. Cytokine & growth factor reviews 44, 51–68. [PubMed: 30396776]
5. Burns JM, Summers BC, Wang Y, Melikian A, Berahovich R, Miao Z, Penfold ME, Sunshine MJ, Littman DR, Kuo CJ, Wei K, McMaster BE, Wright K, Howard MC, Schall TJ (2006) A novel chemokine receptor for SDF-1 and I-TAC involved in cell survival, cell adhesion, and tumor development. J Exp Med 203, 2201–13. [PubMed: 16940167]
6. Zabel BA, Wang Y, Lewen S, Berahovich RD, Penfold ME, Zhang P, Powers J, Summers BC, Miao Z, Zhao B, Jalili A, Janowska-Wieczorek A, Jaen JC, Schall TJ (2009) Elucidation of CXCR7-mediated signaling events and inhibition of CXCR4-mediated tumor cell transendothelial migration by CXCR7 ligands. J Immunol 183, 3204–11. [PubMed: 19641136]
7. Balabanian K, Lagane B, Infantino S, Chow KY, Harriague J, Moepps B, Arenzana-Seisdedos F, Thelen M, Bachelerie F. (2005) The chemokine SDF-1/CXCL12 binds to and signals through the orphan receptor RDC1 in T lymphocytes. The Journal of biological chemistry 280, 35760–6. [PubMed: 16107333]
8. Koenen J, Bachelerie F, Balabanian K, Schlecht-Louf G, Gallego C. (2019) Atypical chemokine receptor 3 (ACKR3): a comprehensive overview of its expression and potential roles in the immune system. Molecular pharmacology.
9. Miao Z, Luker KE, Summers BC, Berahovich R, Bhojani MS, Rehemtulla A, Kleer CG, Essner JJ, Nasevicius A, Luker GD, Howard MC, Schall TJ (2007) CXCR7 (RDC1) promotes breast and lung tumor growth in vivo and is expressed on tumor-associated vasculature. Proceedings of the National Academy of Sciences of the United States of America 104, 15735–40. [PubMed: 17898181]
10. Zheng K, Li HY, Su XL, Wang XY, Tian T, Li F, Ren GS (2010) Chemokine receptor CXCR7 regulates the invasion, angiogenesis and tumor growth of human hepatocellular carcinoma cells. Journal of experimental & clinical cancer research : CR 29, 31. [PubMed: 20380740]
11. Zabel BA, Lewen S, Berahovich RD, Jaen JC, Schall TJ (2011) The novel chemokine receptor CXCR7 regulates trans-endothelial migration of cancer cells. Molecular cancer 10, 73. [PubMed: 21672222]
12. Sierro F, Biben C, Martinez-Munoz L, Mellado M, Ransohoff RM, Li M, Woehl B, Leung H, Groom J, Batten M, Harvey RP, Martinez AC, Mackay CR, Mackay F. (2007) Disrupted cardiac development but normal hematopoiesis in mice deficient in the second CXCL12/SDF-1 receptor, CXCR7. Proceedings of the National Academy of Sciences of the United States of America 104, 14759–64. [PubMed: 17804806]
13. Gerrits H, van Ingen Schenau DS, Bakker NE, van Disseldorp AJ, Strik A, Hermens LS, Koenen TB, Krajnc-Franken MA, Gossen JA (2008) Early postnatal lethality and cardiovascular defects in CXCR7-deficient mice. Genesis 46, 235–45. [PubMed: 18442043]

14. Yu S, Crawford D, Tsuchihashi T, Behrens TW, Srivastava D. (2011) The chemokine receptor CXCR7 functions to regulate cardiac valve remodeling. Developmental dynamics : an official publication of the American Association of Anatomists 240, 384–93. [PubMed: 21246655]
15. Levoye A, Balabanian K, Baleux F, Bachelerie F, Lagane B. (2009) CXCR7 heterodimerizes with CXCR4 and regulates CXCL12-mediated G protein signalling. Blood.
16. Rajagopal S, Kim J, Ahn S, Craig S, Lam CM, Gerard NP, Gerard C, Lefkowitz RJ (2010) Beta-arrestin- but not G protein-mediated signaling by the "decoy" receptor CXCR7. Proceedings of the National Academy of Sciences of the United States of America 107, 628–32. [PubMed: 20018651]
17. Valentin G, Haas P, Gilmour D. (2007) The chemokine SDF1a coordinates tissue migration through the spatially restricted activation of Cxcr7 and Cxcr4b. Curr Biol 17, 1026–31. [PubMed: 17570670]
18. Dambly-Chaudiere C, Cubedo N, Ghysen A. (2007) Control of cell migration in the development of the posterior lateral line: antagonistic interactions between the chemokine receptors CXCR4 and CXCR7/RDC1. BMC Dev Biol 7, 23. [PubMed: 17394634]
19. Boldajipour B, Mahabaleshwar H, Kardash E, Reichman-Fried M, Blaser H, Minina S, Wilson D, Xu Q, Raz E. (2008) Control of chemokine-guided cell migration by ligand sequestration. Cell 132, 463–73. [PubMed: 18267076]
20. Luker KE, Lewin SA, Mihalko LA, Schmidt BT, Winkler JS, Coggins NL, Thomas DG, Luker GD (2012) Scavenging of CXCL12 by CXCR7 promotes tumor growth and metastasis of CXCR4-positive breast cancer cells. Oncogene 31, 4750–8. [PubMed: 22266857]
21. Naumann U, Cameroni E, Pruenster M, Mahabaleshwar H, Raz E, Zerwes HG, Rot A, Thelen M. (2010) CXCR7 functions as a scavenger for CXCL12 and CXCL11. PloS one 5, e9175.
22. Saaber F, Schutz D, Miess E, Abe P, Desikan S, Ashok Kumar P, Balk S, Huang K, Beaulieu JM, Schulz S, Stumm R. (2019) ACKR3 Regulation of Neuronal Migration Requires ACKR3 Phosphorylation, but Not beta-Arrestin. Cell reports 26, 1473–1488 e9. [PubMed: 30726732]
23. Decaillot FM, Kazmi MA, Lin Y, Ray-Saha S, Sakmar TP, Sachdev P. (2011) CXCR7/CXCR4 heterodimer constitutively recruits beta-arrestin to enhance cell migration. The Journal of biological chemistry 286, 32188–97. [PubMed: 21730065]
24. Luker KE, Gupta M, Luker GD (2009) Imaging chemokine receptor dimerization with firefly luciferase complementation. FASEB journal : official publication of the Federation of American Societies for Experimental Biology 23, 823–34. [PubMed: 19001056]
25. Wu B, Chien EY, Mol CD, Fenalti G, Liu W, Katritch V, Abagyan R, Brooun A, Wells P, Bi FC, Hamel DJ, Kuhn P, Handel TM, Cherezov V, Stevens RC (2010) Structures of the CXCR4 chemokine GPCR with small-molecule and cyclic peptide antagonists. Science 330, 1066–71. [PubMed: 20929726]
26. Singer II, Scott S, Kawka DW, Chin J, Daugherty BL, DeMartino JA, DiSalvo J, Gould SL, Lineberger JE, Malkowitz L, Miller MD, Mitnaul L, Siciliano SJ, Staruch MJ, Williams HR, Zweerink HJ, Springer MS (2001) CCR5, CXCR4, and CD4 are clustered and closely apposed on microvilli of human macrophages and T cells. Journal of virology 75, 3779–90. [PubMed: 11264367]
27. Martinez-Munoz L, Rodriguez-Frade JM, Barroso R, Sorzano COS, Torreno-Pina JA, Santiago CA, Manzo C, Lucas P, Garcia-Cuesta EM, Gutierrez E, Barrio L, Vargas J, Cascio G, Carrasco YR, Sanchez-Madrid F, Garcia-Parajo MF, Mellado M. (2018) Separating Actin-Dependent Chemokine Receptor Nanoclustering from Dimerization Indicates a Role for Clustering in CXCR4 Signaling and Function. Molecular cell 71, 873.
28. Crump MP, Gong JH, Loetscher P, Rajarathnam K, Amara A, Arenzana-Seisdedos F, Virelizier JL, Baggiolini M, Sykes BD, Clark-Lewis I. (1997) Solution structure and basis for functional activity of stromal cell-derived factor-1; dissociation of CXCR4 activation from binding and inhibition of HIV-1. Embo J 16, 6996–7007. [PubMed: 9384579]
29. Kufareva I, Gustavsson M, Zheng Y, Stephens BS, Handel TM (2017) What Do Structures Tell Us About Chemokine Receptor Function and Antagonism? Annual review of biophysics 46, 175–198.
30. Ziarek JJ, Kleist AB, London N, Raveh B, Montpas N, Bonneterre J, St-Onge G, DiCosmo-Ponticello CJ, Koplinski CA, Roy I, Stephens B, Thelen S, Veldkamp CT, Coffman FD, Cohen MC, Dwinell MB, Thelen M, Peterson FC, Heveker N, Volkman BF (2017) Structural basis for

chemokine recognition by a G protein-coupled receptor and implications for receptor activation. Science signaling 10.

31. Qin L, Kufareva I, Holden LG, Wang C, Zheng Y, Zhao C, Fenalti G, Wu H, Han GW, Cherezov V, Abagyan R, Stevens RC, Handel TM (2015) Structural biology. Crystal structure of the chemokine receptor CXCR4 in complex with a viral chemokine. Science 347, 1117–22. [PubMed: 25612609]
32. Kufareva I, Stephens BS, Holden LG, Qin L, Zhao C, Kawamura T, Abagyan R, Handel TM (2014) Stoichiometry and geometry of the CXC chemokine receptor 4 complex with CXC ligand 12: molecular modeling and experimental validation. Proceedings of the National Academy of Sciences of the United States of America 111, E5363–72. [PubMed: 25468967]
33. Heveker N, Montes M, Germeroth L, Amara A, Trautmann A, Alizon M, Schneider-Mergener J. (1998) Dissociation of the signalling and antiviral properties of SDF-1-derived small peptides. Curr Biol 8, 369–76. [PubMed: 9545196]
34. Kofuku Y, Yoshiura C, Ueda T, Terasawa H, Hirai T, Tominaga S, Hirose M, Maeda Y, Takahashi H, Terashima Y, Matsushima K, Shimada I. (2009) Structural basis of the interaction between chemokine stromal cell-derived factor-1/CXCL12 and its G-protein-coupled receptor CXCR4. The Journal of biological chemistry 284, 35240–50. [PubMed: 19837984]
35. Veldkamp CT, Seibert C, Peterson FC, De la Cruz NB, Haugner JC 3rd, Basnet H, Sakmar TP, Volkman BF (2008) Structural basis of CXCR4 sulfotyrosine recognition by the chemokine SDF-1/CXCL12. Science signaling 1, ra4.
36. Szpakowska M, Nevins AM, Meyrath M, Rhainds D, D'Huys T, Guite-Vinet F, Dupuis N, Gauthier PA, Counson M, Kleist A, St-Onge G, Hanson J, Schols D, Volkman BF, Heveker N, Chevigne A. (2018) Different contributions of chemokine N-terminal features attest to a different ligand binding mode and a bias towards activation of ACKR3/CXCR7 compared with CXCR4 and CXCR3. British journal of pharmacology 175, 1419–1438. [PubMed: 29272550]
37. Gustavsson M, Wang L, van Gils N, Stephens BS, Zhang P, Schall TJ, Yang S, Abagyan R, Chance MR, Kufareva I, Handel TM (2017) Structural basis of ligand interaction with atypical chemokine receptor 3. Nature communications 8, 14135.
38. Loetscher P, Gong JH, Dewald B, Baggiolini M, Clark-Lewis I. (1998) N-terminal peptides of stromal cell-derived factor-1 with CXC chemokine receptor 4 agonist and antagonist activities. The Journal of biological chemistry 273, 22279–83. [PubMed: 9712844]
39. Vergote D, Butler GS, Ooms M, Cox JH, Silva C, Hollenberg MD, Jhamandas JH, Overall CM, Power C. (2006) Proteolytic processing of SDF-1alpha reveals a change in receptor specificity mediating HIV-associated neurodegeneration. Proceedings of the National Academy of Sciences of the United States of America 103, 19182–7. [PubMed: 17148615]
40. Amara A, Lorthioir O, Valenzuela A, Magerus A, Thelen M, Montes M, Virelizier JL, Delepierre M, Baleux F, Lortat-Jacob H, Arenzana-Seisdedos F. (1999) Stromal cell-derived factor-1alpha associates with heparan sulfates through the first beta-strand of the chemokine. The Journal of biological chemistry 274, 23916–25. [PubMed: 10446158]
41. Scott MG, Pierotti V, Storez H, Lindberg E, Thuret A, Muntaner O, Labbe-Jullie C, Pitcher JA, Marullo S. (2006) Cooperative regulation of extracellular signal-regulated kinase activation and cell shape change by filamin A and beta-arrestins. Mol Cell Biol 26, 3432–45. [PubMed: 16611986]
42. Kamal M, Marquez M, Vauthier V, Leloire A, Froguel P, Jockers R, Couturier C. (2009) Improved donor/acceptor BRET couples for monitoring beta-arrestin recruitment to G protein-coupled receptors. Biotechnol J 4, 1337–44. [PubMed: 19557797]
43. Zwier JM, Roux T, Cottet M, Durroux T, Douzon S, Bdioui S, Gregor N, Bourrier E, Oueslati N, Nicolas L, Tinel N, Boisseau C, Yverneau P, Charrier-Savournin F, Fink M, Trinquet E. (2010) A fluorescent ligand-binding alternative using Tag-lite(R) technology. J Biomol Screen 15, 1248–59. [PubMed: 20974902]
44. Levoye A, Zwier JM, Jaracz-Ros A, Klipfel L, Cottet M, Maurel D, Bdioui S, Balabanian K, Prezeau L, Trinquet E, Durroux T, Bachelerie F. (2015) A Broad G Protein-Coupled Receptor Internalization Assay that Combines SNAP-Tag Labeling, Diffusion-Enhanced Resonance Energy Transfer, and a Highly Emissive Terbium Cryptate. Frontiers in endocrinology 6, 167. [PubMed: 26617570]

45. Pettersen EF, Goddard TD, Huang CC, Couch GS, Greenblatt DM, Meng EC, Ferrin TE (2004) UCSF Chimera--a visualization system for exploratory research and analysis. Journal of computational chemistry 25, 1605–12. [PubMed: 15264254]
46. SOLVATE is written by Helmut Grubmüller, Theoretical Biophysics Group, Institut für Medizinische Optik, Ludwig-Maximilians-Universität München, München, Germany.
47. Humphrey W, Dalke A, Schulten K. (1996) VMD: visual molecular dynamics. Journal of molecular graphics 14, 33–8, 27–8. [PubMed: 8744570]
48. MacKerell AD, Bashford D, Bellott M, Dunbrack RL, Evanseck JD, Field MJ, Fischer S, Gao J, Guo H, Ha S, Joseph-McCarthy D, Kuchnir L, Kuczera K, Lau FT, Mattos C, Michnick S, Ngo T, Nguyen DT, Prodhom B, Reiher WE, Roux B, Schlenkrich M, Smith JC, Stote R, Straub J, Watanabe M, Wiorkiewicz-Kuczera J, Yin D, Karplus M. (1998) All-atom empirical potential for molecular modeling and dynamics studies of proteins. The journal of physical chemistry. B 102, 3586–616. [PubMed: 24889800]
49. Mackerell AD Jr., Feig M, Brooks CL 3rd (2004) Extending the treatment of backbone energetics in protein force fields: limitations of gas-phase quantum mechanics in reproducing protein conformational distributions in molecular dynamics simulations. Journal of computational chemistry 25, 1400–15. [PubMed: 15185334]
50. Feller SE, Gawrisch K, MacKerell AD Jr. (2002) Polyunsaturated fatty acids in lipid bilayers: intrinsic and environmental contributions to their unique physical properties. Journal of the American Chemical Society 124, 318–26. [PubMed: 11782184]
51. Feller SE, Zhang Y, Pastor RW, Brooks BR (1995) Constant pressure molecular dynamics simulation: The Langevin piston method. The Journal of Chemical Physics 103, 4613–4621.
52. Jorgensen WL, Chandrasekhar J, Madura JD, Impey RW, Klein ML (1983) Comparison of simple potential functions for simulating liquid water. The Journal of Chemical Physics 79, 926–935.
53. Martyna GJ, Tobias DJ, Klein ML (1994) Constant pressure molecular dynamics algorithms. The Journal of Chemical Physics 101, 4177–4189.
54. Phillips JC, Braun R, Wang W, Gumbart J, Tajkhorshid E, Villa E, Chipot C, Skeel RD, Kale L, Schulten K. (2005) Scalable molecular dynamics with NAMD. Journal of computational chemistry 26, 1781–802. [PubMed: 16222654]
55. NAMD was developed by the Theoretical and Computational Biophysics Group in the Beckman Institute for Advanced Science and Technology at the University of Illinois at Urbana-Champaign.
56. Hanes MS, Salanga CL, Chowdry AB, Comerford I, McColl SR, Kufareva I, Handel TM (2015) Dual targeting of the chemokine receptors CXCR4 and ACKR3 with novel engineered chemokines. The Journal of biological chemistry 290, 22385–97. [PubMed: 26216880]
57. McQuibban GA, Butler GS, Gong JH, Bendall L, Power C, Clark-Lewis I, Overall CM (2001) Matrix metalloproteinase activity inactivates the CXC chemokine stromal cell-derived factor-1. The Journal of biological chemistry 276, 43503–8. [PubMed: 11571304]
58. Kenakin T. (2011) Functional selectivity and biased receptor signaling. The Journal of pharmacology and experimental therapeutics 336, 296–302. [PubMed: 21030484]
59. Galandrin S and Bouvier M. (2006) Distinct signaling profiles of beta1 and beta2 adrenergic receptor ligands toward adenylyl cyclase and mitogen-activated protein kinase reveals the pluridimensionality of efficacy. Molecular pharmacology 70, 1575–84. [PubMed: 16901982]
60. Cheng ZJ, Zhao J, Sun Y, Hu W, Wu YL, Cen B, Wu GX, Pei G. (2000) beta-arrestin differentially regulates the chemokine receptor CXCR4-mediated signaling and receptor internalization, and this implicates multiple interaction sites between beta-arrestin and CXCR4. J Biol Chem 275, 2479–85. [PubMed: 10644702]
61. Benredjem B, Girard M, Rhainds D, St-Onge G, Heveker N. (2017) Mutational Analysis of Atypical Chemokine Receptor 3 (ACKR3/CXCR7) Interaction with Its Chemokine Ligands CXCL11 and CXCL12. The Journal of biological chemistry 292, 31–42. [PubMed: 27875312]
62. Charest PG, Terrillon S, Bouvier M. (2005) Monitoring agonist-promoted conformational changes of beta-arrestin in living cells by intramolecular BRET. EMBO reports 6, 334–40. [PubMed: 15776020]

63. Ballesteros JA and Weinstein H. (1995) [19] Integrated methods for the construction of three-dimensional models and computational probing of structure-function relations in G protein-coupled receptors. 25, 366–428.

64. Gustavsson M, Dyer DP, Zhao C, Handel TM (2019) Kinetics of CXCL12 binding to atypical chemokine receptor 3 reveal a role for the receptor N terminus in chemokine binding. Science signaling 12.

65. Janssens R, Mortier A, Boff D, Ruytinx P, Gouwy M, Vantilt B, Larsen O, Daugvilaite V, Rosenkilde MM, Parmentier M, Noppen S, Liekens S, Van Damme J, Struyf S, Teixeira MM, Amaral FA, Proost P. (2017) Truncation of CXCL12 by CD26 reduces its CXC chemokine receptor 4- and atypical chemokine receptor 3-dependent activity on endothelial cells and lymphocytes. Biochemical pharmacology 132, 92–101. [PubMed: 28322746]

66. Loetscher P and Clark-Lewis I. (2001) Agonistic and antagonistic activities of chemokines. Journal of leukocyte biology 69, 881–4. [PubMed: 11404371]

67. Proost P, Struyf S, Schols D, Durinx C, Wuyts A, Lenaerts JP, De Clercq E, De Meester I, Van Damme J. (1998) Processing by CD26/dipeptidyl-peptidase IV reduces the chemotactic and anti-HIV-1 activity of stromal-cell-derived factor-1alpha. FEBS letters 432, 73–6. [PubMed: 9710254]

68. Canals M, Scholten DJ, de Munnik S, Han MK, Smit MJ, Leurs R. (2012) Ubiquitination of CXCR7 controls receptor trafficking. PloS one 7, e34192.

Chemokine	Sequence
CXCL12	KPVSLSYRCPCRFFE
CXCL12 K1R	**R**PVSLSYRCPCRFFE
CXCL12 P2G	K**G**VSLSYRCPCRFFE
CXCL12 4-67	- - - SLSYRCPCRFFE
CXCL12 5-67	- - - - LSYRCPCRFFE

FIGURE 1. Sequences of the first 15 N-terminal residues of WT CXCL12 and the four CXCL12 variants.

Substitution of Lysine 1 (K1) and Proline 2 (P2) in CXCL12 WT are highlighted in bold.

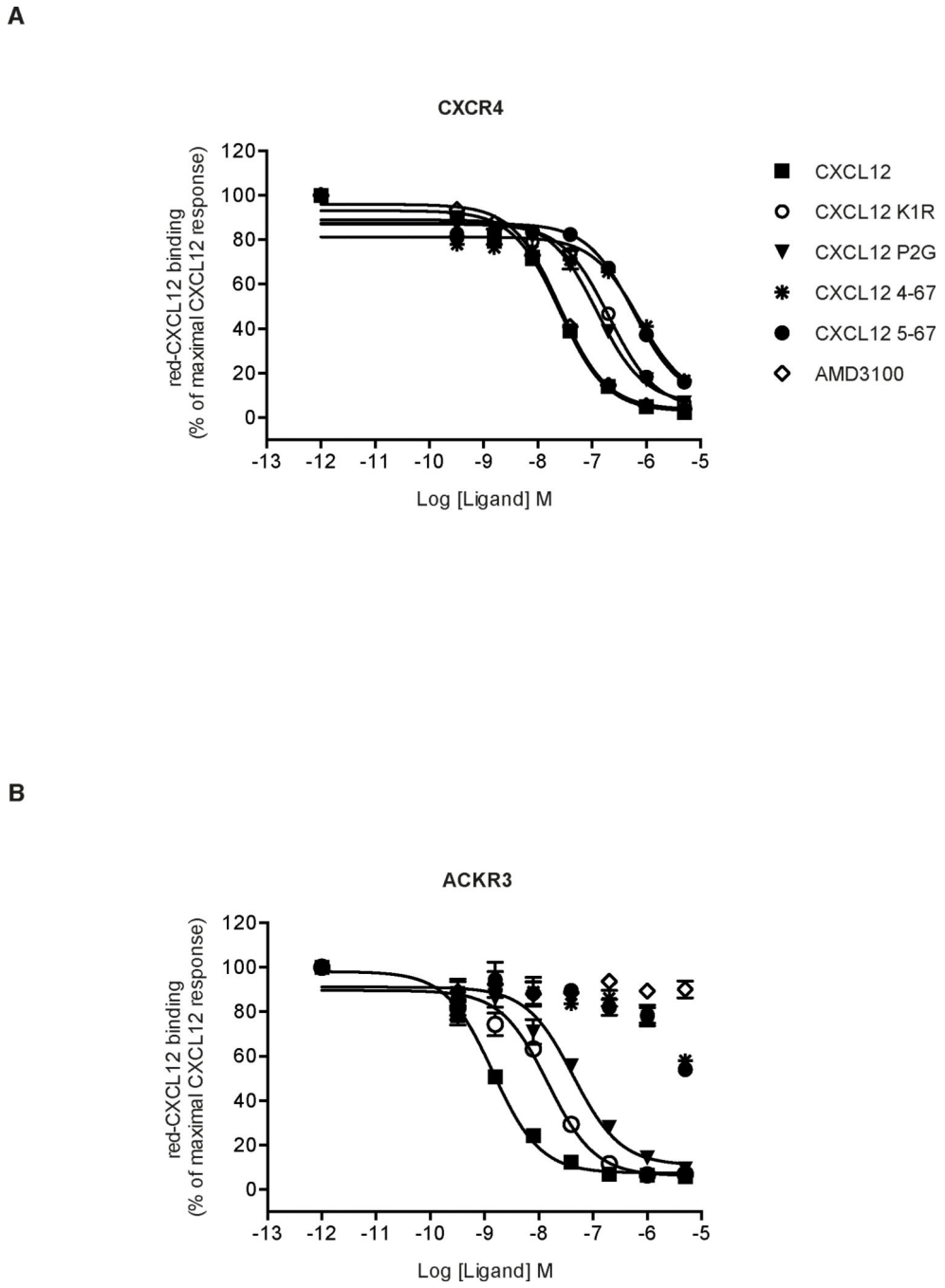

FIGURE 2. CXCL12 N-terminal variants differentially bind to CXCR4 and ACKR3.

HTRF-based competition experiments performed in CXCR4-expressing (A) and ACKR3-expressing (B) HEK293 cells incubated in the presence of red-CXCL12 and the indicated concentrations of ligands. Values are mean ±SEM of four experiments, each performed in triplicate expressed as percent of the maximal binding obtained without competitor.

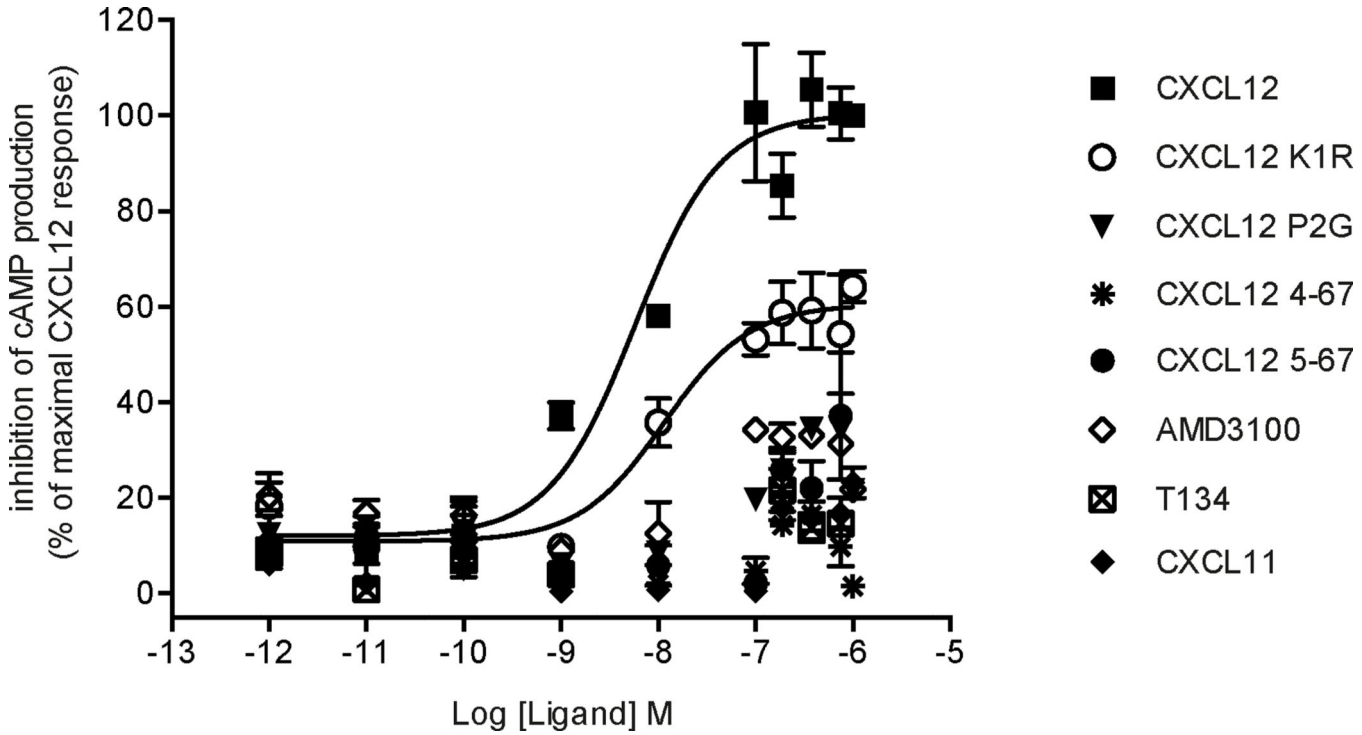

FIGURE 3. Inhibition of cAMP production induced by CXCL12 variants.

cAMP levels were accessed by HTRF-based assays in ST-CXCR4 cells treated with forskolin and stimulated with increasing concentrations of the indicated ligands. HTRF ratios were plotted as a function of ligand concentrations normalized to the maximal response to 1 μM WT CXCL12, and expressed as inhibition of cAMP production (% of maximal CXCL12 response). Data represent the mean ±SEM of two experiments performed in triplicate.

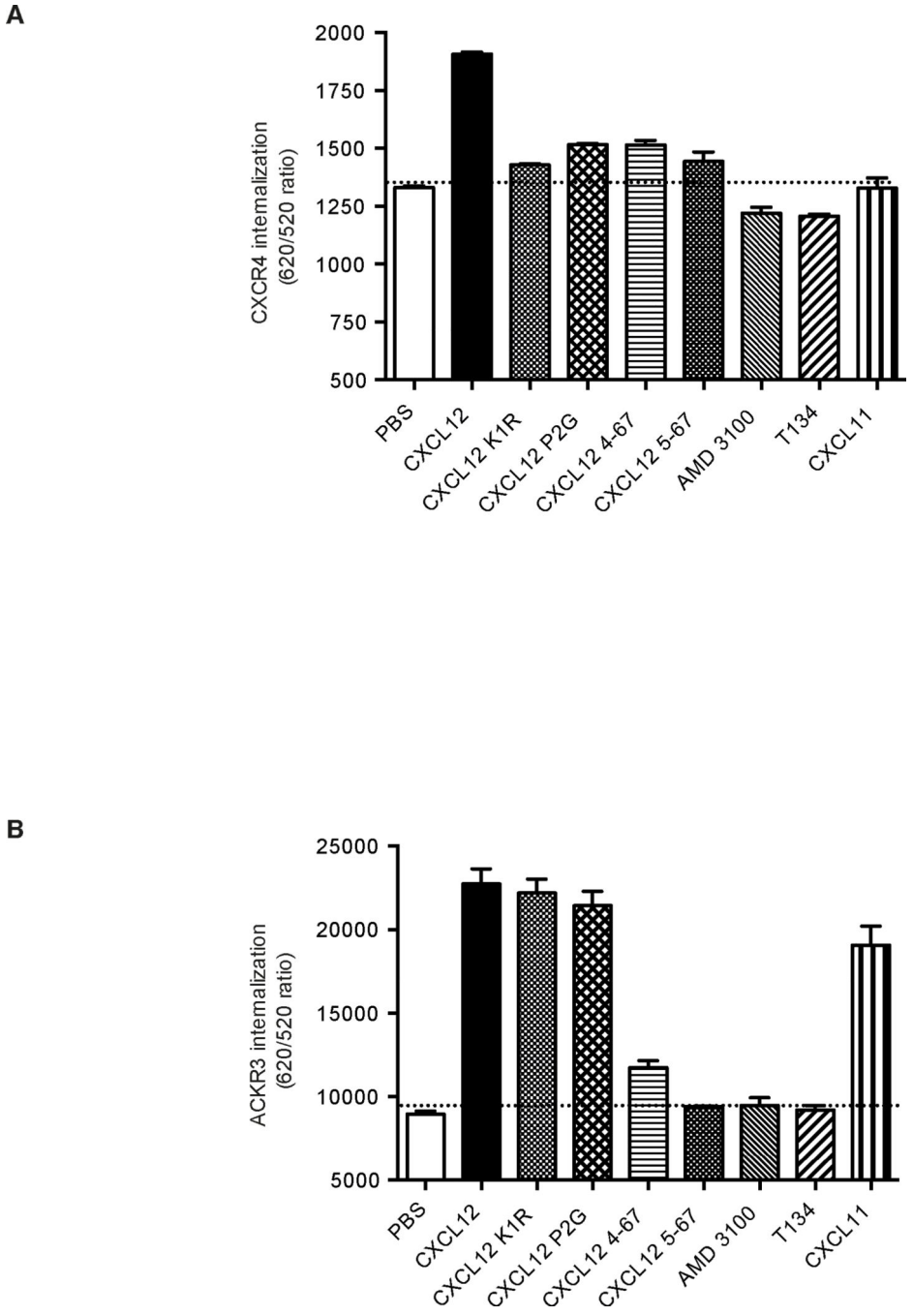

FIGURE 4. Effect of CXCL12 variants on receptor internalization.

Cells stably expressing ST-CXCR4 (A) or ST-ACKR3 (B) receptors and labeled with SNAP-Lumi4Tb fluorescent substrate were incubated in medium (PBS) or in the presence of the indicated ligands (1 μM). Results represent the mean ±SEM of two independent experiments performed in triplicate. The thresholds corresponding to the signal without ligand are shown (black dashed line).

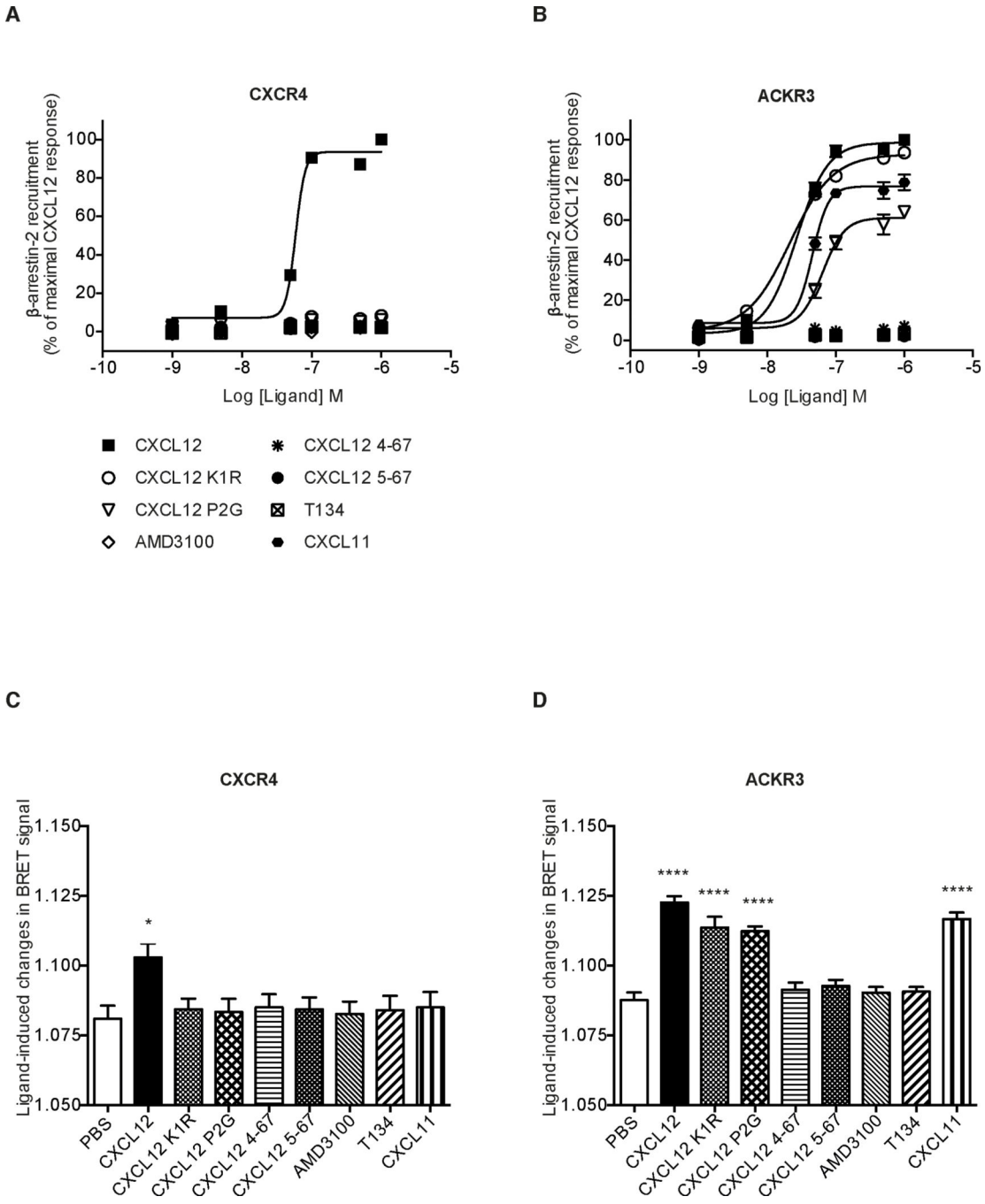

FIGURE 5. CXCL12 variants differentially induce β-arrestin 2 recruitment to the two receptors and receptor-dependent β-arrestin 2 activation.

HEK293T cells were transiently co-transfected with Rluc-β-arrestin 2 and CXCR4-YFP (A) or Rluc-β-arrestin 2 and ACKR3-YFP (B) and stimulated with increasing concentrations of the indicated ligands. BRET data were expressed as percent of the maximal response induced by 1 μM of WT CXCL12. Data represent the mean ±SEM of three independent experiments performed in duplicate. (C-D) Intramolecular BRET assay to monitor receptor-dependent β-arrestin 2 activation. Ligand-promoted conformational changes of β-arrestin 2 were monitored by using Rluc8-β-arrestin 2-Ypet in CXCR4 (C) or ACKR3 (D) transfected

cells stimulated by the indicated ligands (1 μM). Data represent the mean ±SEM of three independent experiments performed in duplicate.

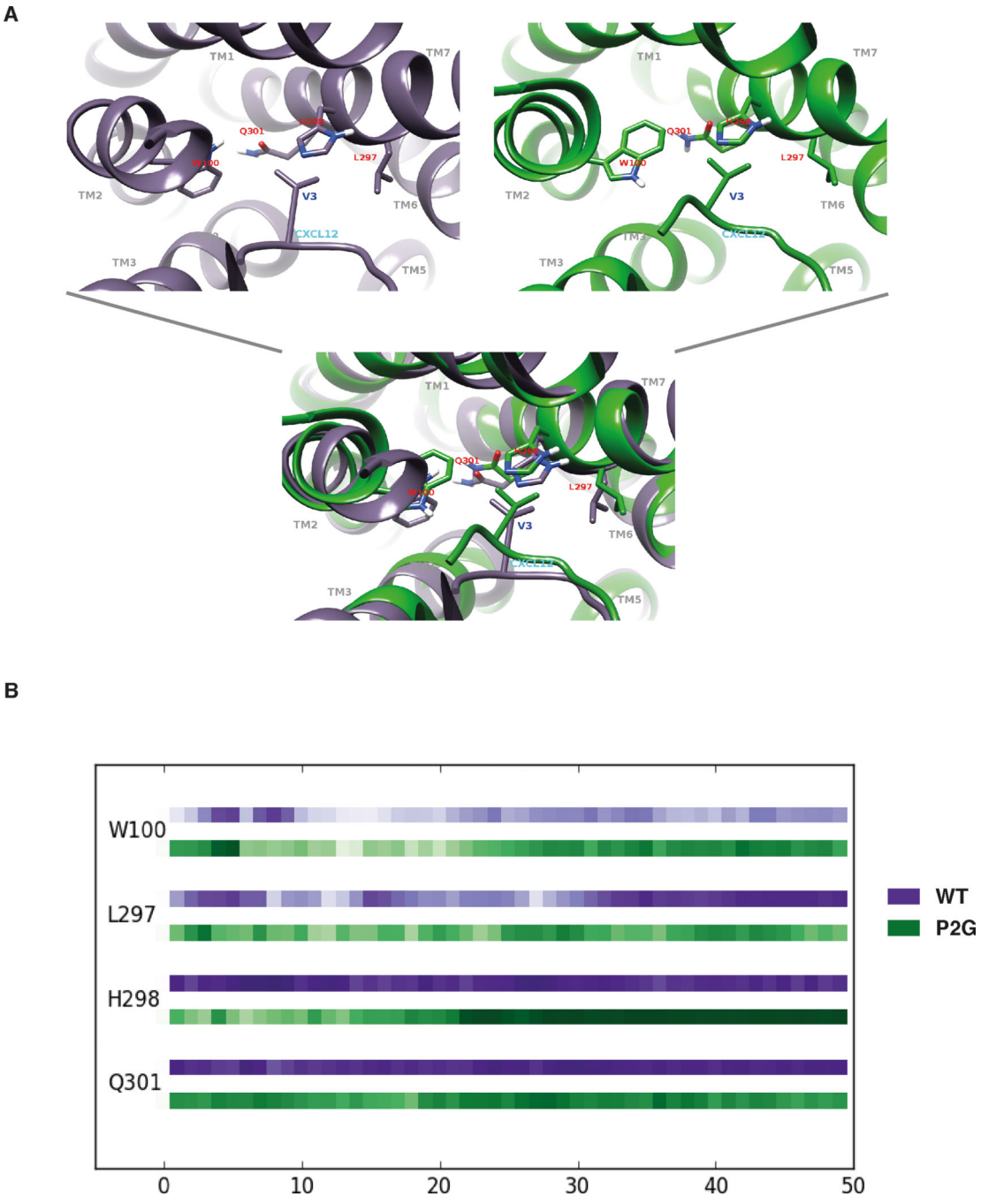

FIGURE 6. MD simulations of ACKR3-CXCL12 complexes revealed a critical role for the V3 N-terminal residue of CXCL12.

(A) Views of the interaction sites established between ACKR3 residues (marked in red) and the V3 residue of either the WT CXCL12 (left panel) or the P2G variant (right panel). Bottom panel represents a superposition of both tertiary structures. (B) Plots of the interaction strength between the V3 residue of either CXCL12 (purple line) or the P2G variant (green line) and ACKR3 residues as a function of time. ACKR3 residues are listed on the left side of the chronogram and the horizontal axis corresponds to the time of

simulation in ns. Interaction strength is represented as a function of color intensity (darker color indicates stronger interaction).

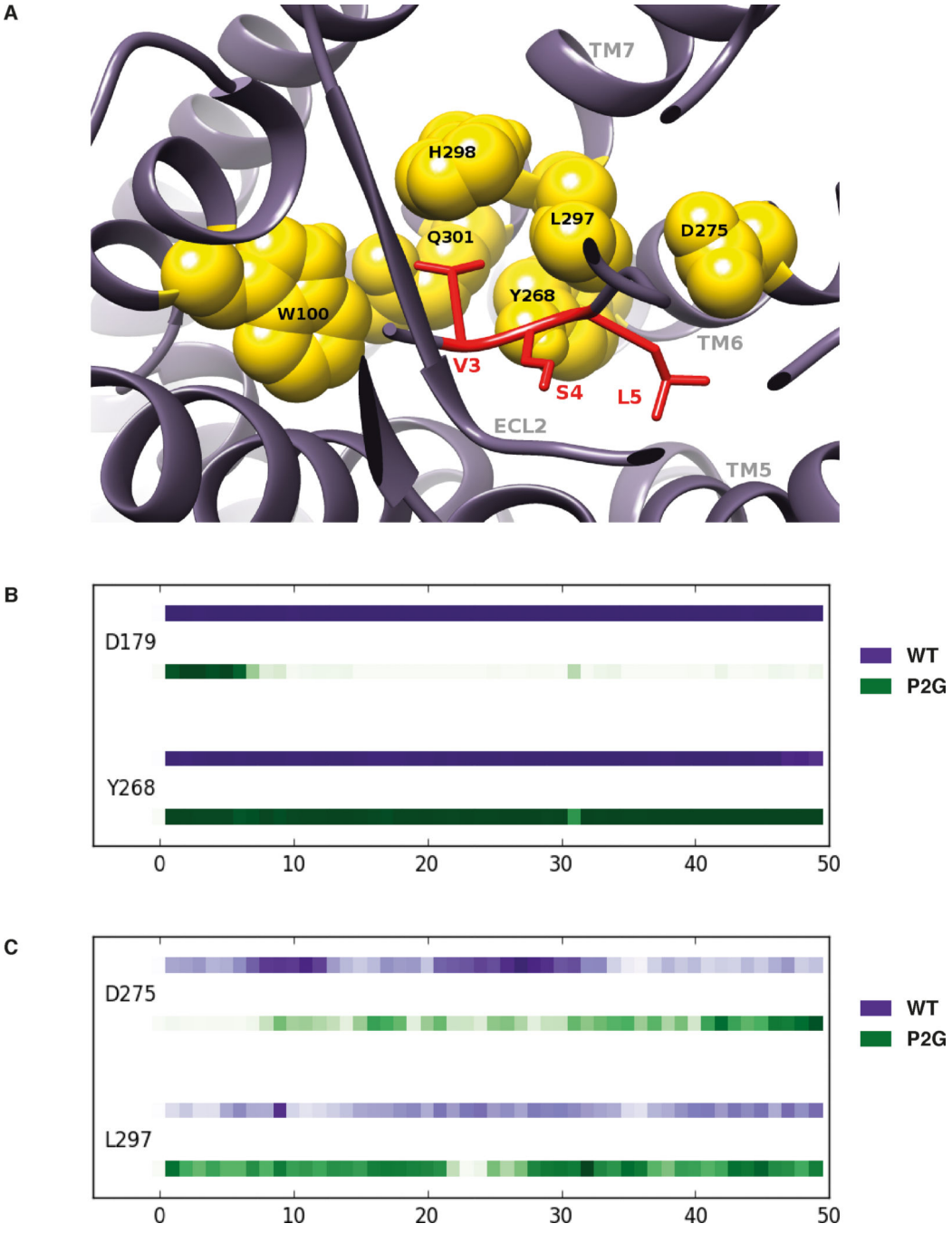

FIGURE 7. Interactions of N-terminal CXCL12 V3, S4 and L5 residues within a binding pocket of ACKR3.

(A) Views of the interaction sites established between ACKR3 residues (yellow sphere) and the V3, S4 and L5 residues of the WT CXCL12 (marked in red). (B-C) Plots of the interactions strength established between the S4 (B) and L5 (C) residues of either WT CXCL12 (purple line) or the P2G variant (green line) and ACKR3 residues as a function of time. ACKR3 residues are listed on the left side of the chronogram and horizontal axis

corresponds to the time of simulation in ns. Interaction strength is represented as a function of color intensity (darker color indicates stronger interaction).

Table 1:

Binding properties of CXCL12 and its variants towards CXCR4 and ACKR3

	CXCR4			ACKR3		
Ligands	**K_d (nM)[a]**	**K_i (nM)[b]**	**pIC_{50}[c]**	**K_d (nM)[a]**	**K_i (nM)[b]**	**pIC_{50}[c]**
CXCL12	22.7 ± 0.7	16.12 ± 0.92	7.61 ± 0.02	1.1± 0.2	0.21 ± 0.02	8.85 ± 0.05
K1R		132.01 ± 6.02	6.47 ± 0.08****		1.91 ± 0.19	7.84 ± 0.04****
P2G		79.96 ± 6.89	6.68 ± 0.17****		7.09 ± 0.40	7.36 ± 0.03****
4–67		470.57 ± 48.36	6.15 ± 0.05****		*d*	*d*
5–67		377.77 ± 28.32	6.23 ± 0.03****		*d*	*d*
AMD3100		16.38 ± 1.44	7.60 ± 0.04		*d*	*d*

[a] K_d values refer to the dissociation constant

[b] K_i values refer to the inhibitory constant

[c] pIC_{50} is the negative logarithm of the half maximal inhibitory concentration (IC_{50}).

pIC_{50} values are the mean ± SEM of three independent experiments performed at least in triplicate. Significantly lowered potency relative to CXCL12 is noted:

**** P<0.0001 from one-way analysis of variance (ANOVA) with Dunnett's multiple comparison test.

[d] Not applicable

Table 2:

Inhibition of cAMP production induced by CXCL12 and its variants

	CXCR4		
Ligands	**IC_{50} (nM)[a]**	**pIC_{50}[b]**	**E_{max}[c] (% CXCL12)**
CXCL12	5.78	8.26 ± 0.23	100
K1R	11.5	7.94 ± 0.09	57.73 ± 3.35***
P2G	*d*	*d*	*d*
4–67	*d*	*d*	*d*
5–67	*d*	*d*	*d*
CXCL11	*d*	*d*	*d*
AMD3100	*d*	*d*	*d*
T134	*d*	*d*	*d*

[a] IC_{50} values refer to the concentrations which induce half-maximal cAMP production inhibition downstream CXCR4.

[b] pIC_{50} values are the mean ± SEM of three independent experiments performed at least in triplicate.

[c] E_{max} values for chemokine variants are shown as a percentage of the maximum values obtained for CXCL12. Significant difference for CXCL12 K1R compared to CXCL12 is noted:

*** $P<0.001$ from unpaired t-test.

[d] Not applicable

Table 3:

Recruitment of β-arrestin 2 induced by CXCL12 and its variants

	CXCR4			ACKR3		
Ligands	**EC_{50} (nM)[a]**	**pEC_{50}[b]**	**E_{max}[c](% CXCL12)**	**EC_{50} (nM)[a]**	**pEC_{50}[b]**	**E_{max}[c](% CXCL12)**
CXCL12	5.78	7.23 ± 0.01	100	26.53	7.58 ± 0.06	100
K1R	*d*	*d*	*d*	22.07	7.66 ± 0.05	92.66 ± 1.39
P2G	*d*	*d*	*d*	*58.99*	7.24 ± 0.08 *	63.33 ± 0.05
4–67	*d*	*d*	*d*	*d*	*d*	*d*
5–67	*d*	*d*	*d*	*d*	*d*	*d*
CXCL11	*d*	*d*	*d*	*d*	*d*	*d*
AMD3100	*d*	*d*	*d*	*d*	*d*	*d*
T134	*d*	*d*	*d*	*d*	*d*	*d*

[a] EC_{50} values (nM) refer to the concentrations which induce half-maximal β-arrestin 2 recruitment downstream ACKR3 and CXCR4.

[b] pEC_{50} (± SEM) were obtained from the nonlinear regression curve of the averaged data.

[c] BRET signal from each ligand were normalized to the maximal response of CXCL12 (%E_{max} of CXCL12). E_{max} was obtained from the response of CXCL12 at a concentration of 1μM. Values are the mean ± SEM of three independent experiments performed at least in triplicate. Significant difference for CXCL12 variant compared to CXCL12 is noted:

* $P<0.05$ from one-way analysis of variance (ANOVA) with Dunnett's multiple comparison test.

[d] Not applicable